DTI^ ℮ COPY

Naval Research Laboratory
Washington, DC 20375-5000

NRL Report 9275

AD-A228 016

High Energy Laser Beam
Pattern Analysis

GEORGE L. HALL

Laser Physics Branch
Optical Sciences Division

August 3, 1990

DTIC
ELECTE
NOV 0 2 1990
S
E
D

90 11 ℮ 0℮3

REPORT DOCUMENTATION PAGE

Form Approved
OMB No 0704-0188

1. AGENCY USE ONLY (Leave blank)	2. REPORT DATE 3 August 1990	3. REPORT TYPE AND DATES COVERED Interim

4. TITLE AND SUBTITLE	5. FUNDING NUMBERS
High Energy Laser Beam Pattern Analysis	PE 65601A TA 145-NRL-D-9 WU F200

6. AUTHOR(S)

Hall, G. L.

7. PERFORMING ORGANIZATION NAME(S) AND ADDRESS(ES)	8. PERFORMING ORGANIZATION REPORT NUMBER
Naval Research Laboratory Washington, DC 20375-5000	NRL Report 9275

9. SPONSORING/MONITORING AGENCY NAME(S) AND ADDRESS(ES)	10. SPONSORING/MONITORING AGENCY REPORT NUMBER
Space and Naval Warfare Systems Command Washington, DC 20363-5100	

11. SUPPLEMENTARY NOTES

12a. DISTRIBUTION/AVAILABILITY STATEMENT	12b. DISTRIBUTION CODE
Approved for public release; distribution unlimited.	

13. ABSTRACT (Maximum 200 words)

Two patterns burned in Plexiglas* by the Mid Infrared Advanced Chemical Laser (MIRACL) were converted to optical images and Fourier transformed optically. One of the patterns was burned before a beam quality upgrade effort, and the other one after. The Fourier spectra were examined for evidence of variations in the laser gain medium and other diffraction sources in the optical system. To date, no specially useful information has been identified from this study, but the technique shows promise for future use under appropriate conditions. The novel method of converting the varying depth of the burn to photographic density is described. This same method could be used to achieve a nonmechanical digitization of a burn pattern for digital image processing.

14. SUBJECT TERMS	15. NUMBER OF PAGES 16
High-energy lasers, Beam pattern, MIRACL	16. PRICE CODE

17. SECURITY CLASSIFICATION OF REPORT	18. SECURITY CLASSIFICATION OF THIS PAGE	19. SECURITY CLASSIFICATION OF ABSTRACT	20. LIMITATION OF ABSTRACT
UNCLASSIFIED	UNCLASSIFIED	UNCLASSIFIED	UL

CONTENTS

By_____
Distribution/_____

Availability Codes

Dist	Avail and/or Special
A-1	

HIGH ENERGY LASER BEAM PATTERN ANALYSIS

INTRODUCTION

Beam diagnostics is one of the more difficult problems in working with high energy lasers. The destructiveness of the beam makes most conventional methods inappropriate. Many of the techniques in use are only partly satisfactory. The cost of operating large lasers limits the time for adjustments while running and deters repetitive trials. Since these difficulties exist, new ideas and techniques are valuable. The subject of this study is diagnostics by the analysis of burn patterns.

Early in the work with lasers at 10.6 µm, Plexiglas® ablation was found to be highly linear with beam intensity. In work at 3.8 µm the transparency upsets the ablation, but Dr. Meyer R. Achter at NRL determined that if the Plexiglas is impregnated with carbon, the linear ablation is restored. The material, Plexiglas G, color 2025, black, is available from Rohm & Hass in quarter-inch sheets and must be laminated to make burn blocks. The burn patterns have allowed experimenters to visually inspect the two-dimensional power pattern of beams and have been especially valuable to workers studying damage and vulnerability to determine peak intensities by taking depth-to-volume ratios. The burns are time averages, but the richness of detail suggests that they are not subject to spatial fluctuations. The technique allows the direct and simple measure of the full power beam-intensity profile.

The first burn pattern from the CW Mid Infrared Advanced Chemical Laser (MIRACL) was made on run HL1-093 of 7 April 1982 at TRW's Capistrano Test Site. Rubber molds of the pattern were made available for study and analysis. At NRL a procedure was sought that would allow Fourier analysis of the pattern. A means for digitizing the pattern was not readily available, so photographic methods were sought for analyzing the pattern in an optical data processor. The technique finally used involved immersing the mold in a colored liquid, in this case tea, and photographing it in such a way that the variation in depth produced a corresponding variation in the density of the film. Figure 1 is the resulting photograph of this first burn pattern. The shape of the beam is determined by the scraper mirror that extracts it from the laser cavity and by the supersonic flow of the gain medium. The scraper mirror has a central rectangular aperture that permits feedback to the unstable resonator. The gain is greatest on the upstream side of the medium and drops off on the downstream side.

OPTICAL PROCESSING OF THE BURN PATTERN

The initial objective of the optical transformation of the burn pattern was twofold. One was to obtain a "best case" far field pattern, assuming that if there were phase variations, that they would tend to make the far field worse rather than better. The other was to obtain spectra that would evidence the presence of periodic wakes in the gain medium, or structure of the optical system. At the time there was much concern for identifying the cause of energy being dispersed from the beam in the vertical dimension, which is orthogonal to the flow and to the optical axis.

The optical processor used consisted of a HeNe laser expanded to flood a transparency of the burn pattern with collimated light and a transforming lens that focused the light on a film holder. The input transparency carrying the image of Fig. 1 was reduced so that the 14-cm height and width of the beam was represented by 4 mm. This combined with the 2.9-m focal length of the system and the 633-nm wavelength of the light source results in a wavelength equal to the width of the beam being represented by 0.45 mm on the film or a wavelength 1/26 the width of the beam being represented by 11.7 mm on the film.
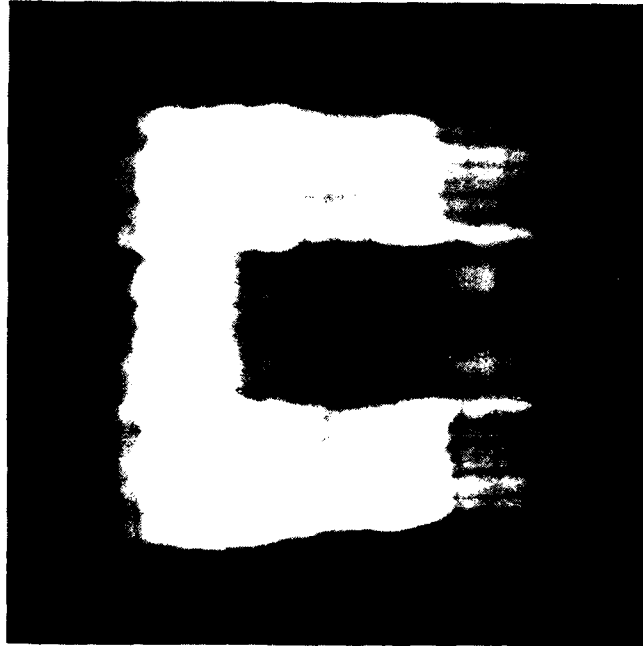
Fig. 1 — The burn pattern made on run HL1-093 of 7 April 1982.
Direction of flow is from left to right.

The spatial frequency spectrum, or far field of the burn pattern, was recorded on film at various exposures as shown in Fig. 2. In Fig. 2(a) the exposure was 1/1000 s, in Fig. 2(b) it was 1/100 s, and so on, so that each exposure was 10 times greater that the previous one. The implication is that 90% of the energy in the spectrum or far field is contained within the area seen in Fig. 2(a) and 99% within the area in Fig. 2(b) and so on. In Fig. 2(a) the center spot is the diffraction limit. The intensity of the light source, length of exposure, threshold of the film, and other factors could not be chosen to delimit the power levels exactly, but the factor of ten ratio of one level to another is fixed by the timing of the exposure. No significant statement about beam quality is intended here since this is a "best case" far field pattern done without consideration of phase effects. However, qualitative information is here in that if the beam were propagated to the far field without thermal blooming or other distorting effects, it would strongly resemble Fig. 2. The greater diffraction along the vertical axis is clearly shown.

Figure 3 shows the analysis of the far field pattern as a frequency spectrum. Here the vertical frequencies are identified as lines per beamwidth or lines per 14 cm. The most prominent of these are identified on the lower half of the figure. One of the highest frequencies identified is 26, which corresponds to the serpentine spacing of the D_2 feed-holes. The feed-holes themselves are a higher frequency that does not appear in the burn pattern. Energy at 3.8 μm diffracted at the feed-hole frequency in a 14-cm-high beam would completely propagate out of the beam in a distance of 33.2 m. The pattern was burned approximately 29.7 m from the cavity scraper mirror. The beam does not leave the cavity as a 14-cm square, but instead it leaves in a tall and narrow form that is squared up by a beam shaping telescope that uses cylindrical mirrors. The result is that in a direction back down the beam from the burn pattern, the vertical edges of the hole in the scraper mirror appear to be 122.2 m away in a virtual image and the horizontal edges appear to be 9.3 m away in a real image. Just before the last cylindrical mirror with a 3.1-m focal length, the beam passes through a horizontal line focus centered in a clipper slit 1.79 cm wide. Acting as a spatial frequency filter, the slit limits the vertical frequencies in the burn pattern to a shortest wavelength of 2.4 mm or 58 lines per beamwidth. Energy diffracted this maximum amount would propagate 3 cm out of the beam in the remaining 11 m to the burn pattern. The spill at the top and bottom of the pattern is of this magnitude.
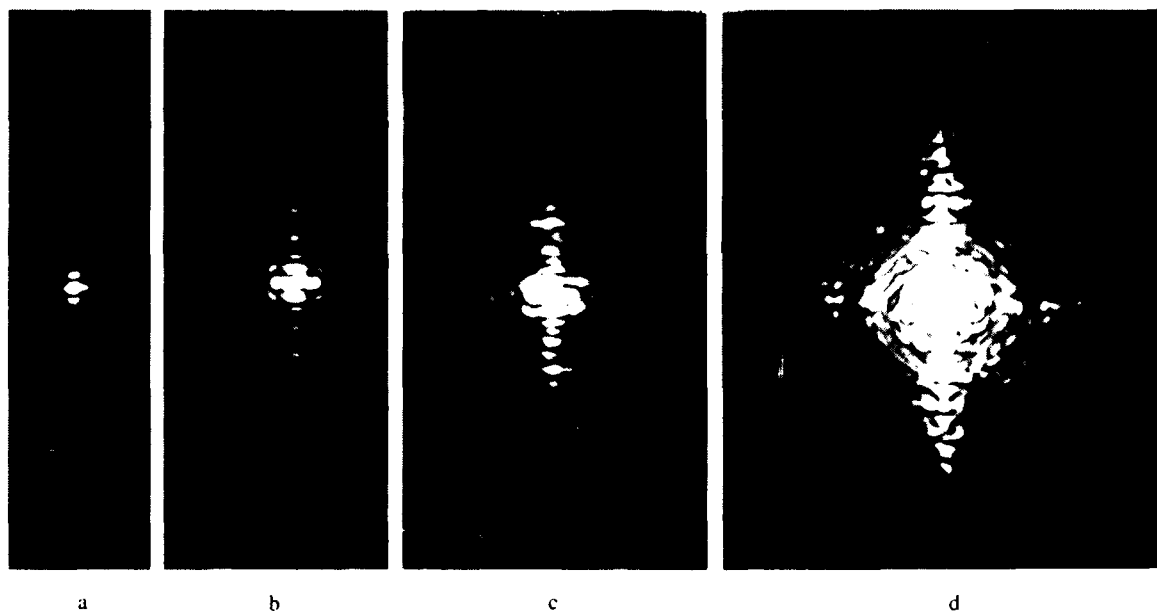
Fig. 2 — The optical Fourier transform of the HL1-093 burn pattern. The photographic exposure increases by a factor of 10 from a to b, b to c, and c to d, with the exposure at d being 1000 times the exposure at a.
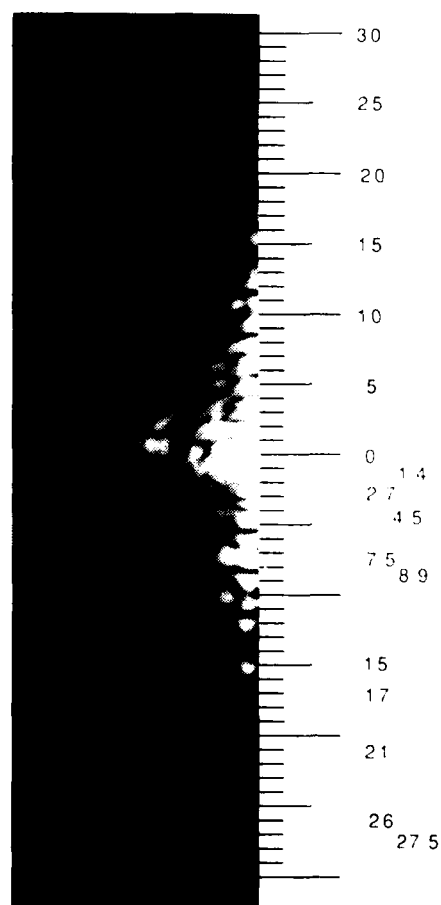

Fig. 3 — The spatial frequencies of the HL1-093 burn pattern in lines per beamwidth. Some of the more prominent frequencies are identified on the lower half of the scale.

HOLOGRAPHIC INTERPRETATION

The burn pattern has the character of a Gabor hologram. To qualify as a Gabor hologram the requirements are that a large amount of undiffracted energy serves as a reference beam and that the amount of diffraction is minor. The near field of the pattern was searched for images of the edges of clippers or even of wakes in the flow, but none was found. The optical system with cylindrical mirrors would prevent all four edges of the hole in the scraper mirror from appearing in a single plane. The images of Gabor holograms are often not that sharp, and the lack of high frequencies would further degrade images of edges, let alone those of fuzzy wakes.

THE BEAM QUALITY UPGRADE

TRW, the MIRACL contractor, and others thoroughly studied the vertical dispersion problem. They concluded that the source of the diffraction was in the gain medium. The buttons that maintain the separation of the blades in the modules had been purposely staggered to avoid alignment of their wakes. It had not seemed necessary to stagger the finer structure of the D_2 feed-holes, and the blade support struts and shock waves from the module shrouds had not been expected to present a problem. The D_2 feed-hole wakes and particularly the feed-hole serpentine wakes were unexpectedly persistent. TRW proposed tilting the module banks as a means of avoiding cumulative index-of-refraction changes along the ray paths caused by alignment with the strut wakes as well as the D_2 wakes. The concept was implemented, and the vertical dispersion was satisfactorily reduced.

Another pattern was burned shortly after the upgrade on run no. ML4 of 10 Jan. 1985. Figure 4 shows the mold from this pattern that was also photographed in tea. Figure 5 shows the optical transform of the pattern. Figure 6 identifies the frequencies in the spectrum. Although the pattern before the upgrade was burned at approximately 29.7 m from the cavity scraper mirror, the one after the upgrade was burned approximately 48.2 m from the scraper. This presents a problem in the comparison of the two.

The spatial frequencies in the burn patterns have two sources. One is the wakes or density variations in the gain medium, and the other is the edges of mirrors or clippers. Just as Gaussians transform to Gaussians, the soft-edged wakes tend to persist in the very near field but the diffraction fringes from the edges become coarser or lower in frequency as they propagate into the near field. See the Appendix. Since the two patterns were burned at different locations in the near field, the fringes from the edges will be different. It would be easier to see the result of the changes in the gain medium if the two patterns had been burned in the same location relative to the diffracting edges of the mirrors and clippers. It would be possible to calculate the diffraction from the edges, but because of the complexity of the MIRACL optical system it would require a more sophisticated code than was available for this analysis.

Fig. 4 — The burn pattern made on run ML4 of 10 Jan. 1985. Direction of flow is from left to right.
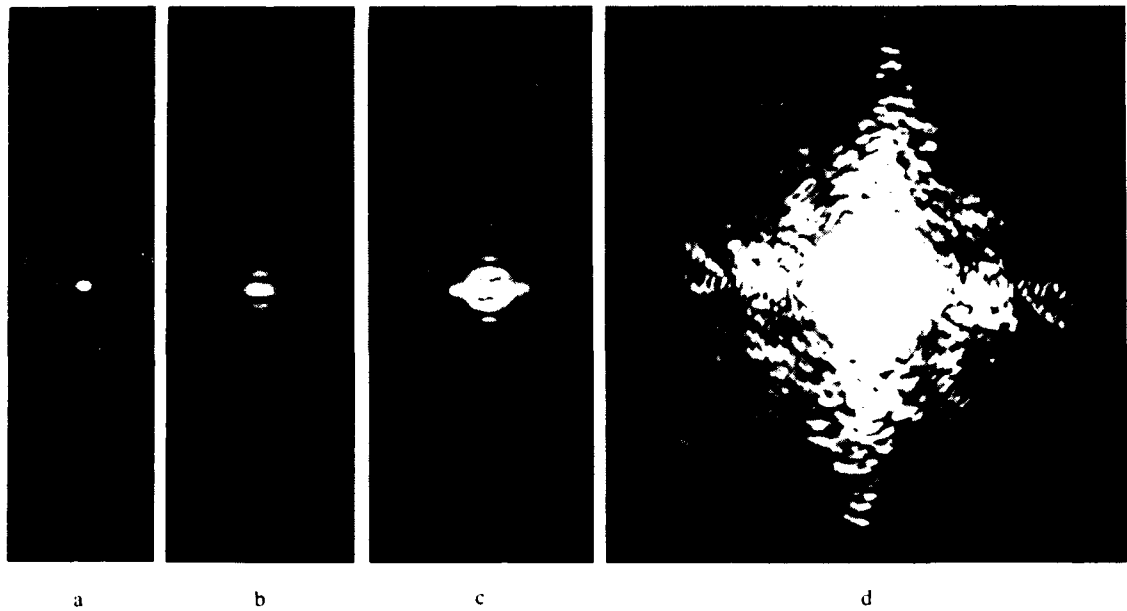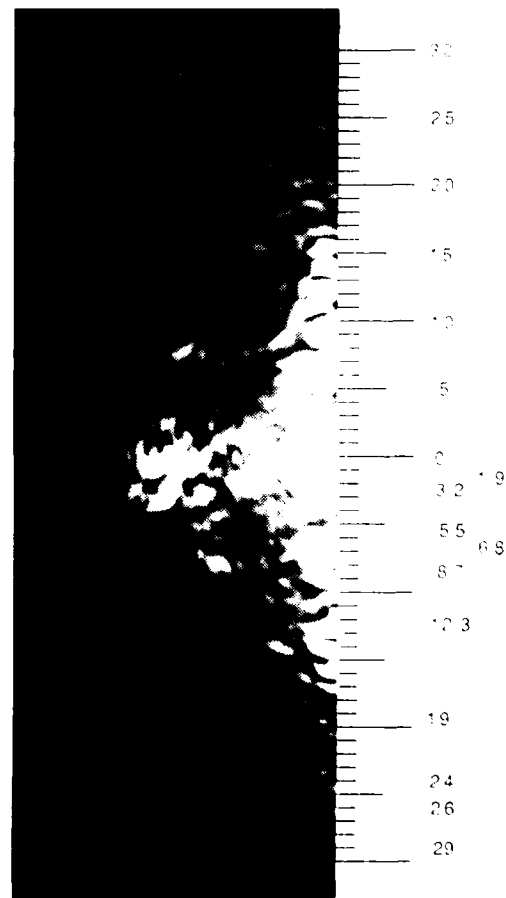
4

Fig. 5 — The optical Fourier transform of the ML4 burn pattern. The photographic exposure increases by a factor of 10 from a to b, b to c, and c to d, with the exposure at d being 1000 times the exposure at a.

Fig. 6 — The spatial frequencies of the ML4 burn pattern in lines per beamwidth. Some of the more prominent frequencies are identified on the lower half of the scale.

THE DIGITIZED BURN PATTERN

Dr. C. D. Bond of NRL's Condensed Matter and Radiation Sciences Division digitized the second burn pattern for use in damage and vulnerability studies. A copy of the raw data was obtained from him so that it might be transformed and compared to the optical transforms.

When the pattern was burned, the beam was cut off by a sliding shutter so that one side received more exposure than the other. The data points were proportionately amplified to compensate for the shutter effect, and Fig. 7 shows the result as a 3-D projection. The data were then transformed by a fast Fourier transform (FFT) routine, and Fig. 8 shows the 3-D projection. Figure 9 shows a vertical slice of the FFT with a logarithmic scale.
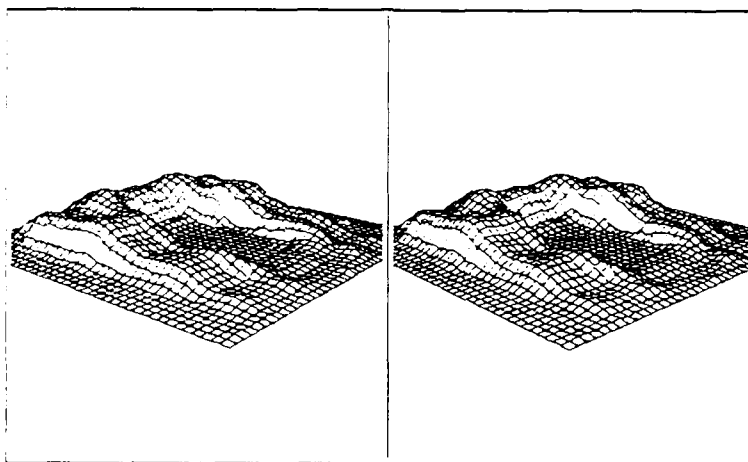

Fig. 7 — Stereo pair of the digitized burn pattern.
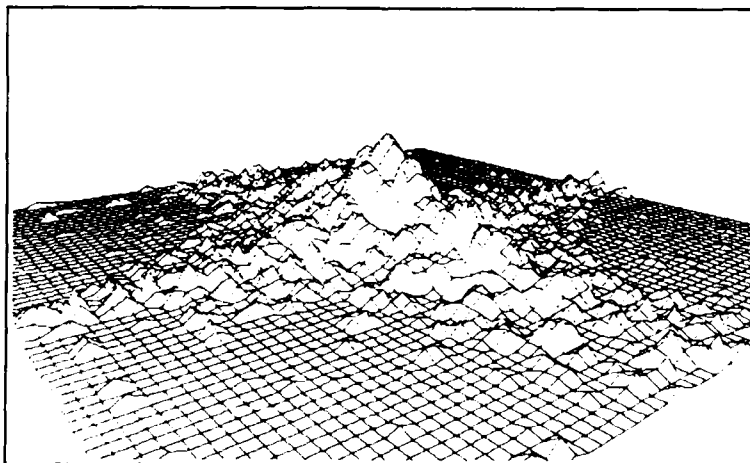The vertical dimension is exaggerated.

Fig. 8 — The FFT of the digitized burn pattern. The vertical scale is logarithmic. The pattern vertical runs from upper left to lower right.
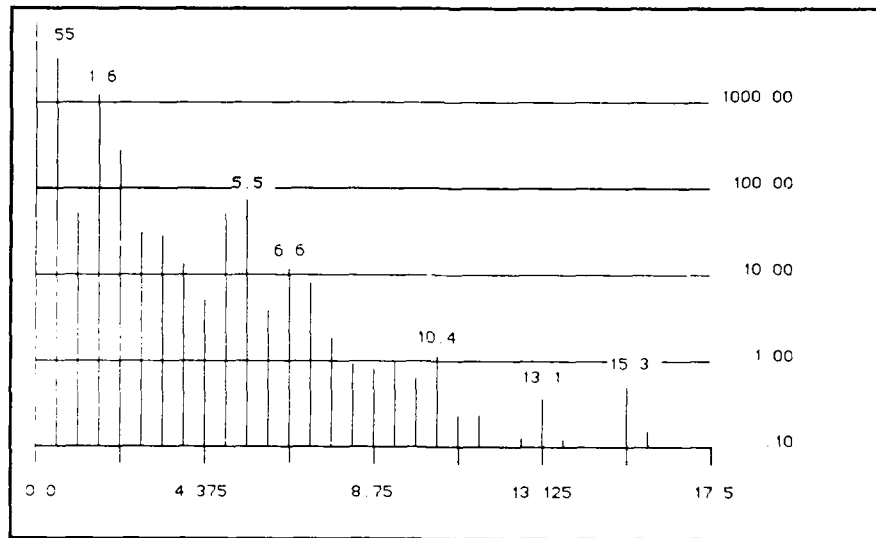
Fig. 9 — A center vertical slice of the FFT of the burn pattern as a spectrum.
The relative intensity of the lines is in arbitrary log units.

Figures 10 and 11 are sketches of what a central vertical slice of the optical transforms of the first and second burns might look like if plotted on a log scale. The spectra were sketched by looking at the shortest exposure and drawing the apparent intensities in the top decade and then proceeding to the next ten times longer exposure and drawing the intensities in the next decade down and so on. The after upgrade spectrum in Fig. 11 might be expected to resemble the spectrum in Fig. 9, but this is not so.

In digitizing the burn, the pattern was sampled every 4 mm or 35 times across a distance of 14 cm. (The sample array was actually 36 x 39.) This made the Nyquist frequency 17.5 lines per 14 cm or a wavelength of 8 mm. Visual inspection of the burn pattern indicates that there are frequencies of shorter wavelength than 8 mm. This means that the sampling of the pattern is not band limited, and these shorter wavelengths will alias as longer wavelengths and give an inaccurate spectrum. Bracewell [1] discusses one-dimensional sampling, and Goodman [2] discusses two-dimensional sampling. The choice of the 4-mm sample rate and a 64 x 64 FFT also means that the FFT spectrum will be expressed in harmonics of 0.546875 lines per 14 cm (35/64), which will also cause some variation in the appearance of the spectrum. The choice of 4 mm as a sample rate was adequate for the automation of volume and intensity calculations for damage and vulnerability studies, but 1 mm or less appears to be required for meaningful spatial frequency analysis of the pattern.

THE OPTICAL TRANSFORM QUALITY

The sample rate of a photograph lies in the grain of the film and often appears as a halo in an optical transform. This should not be confused with the halation that sometimes occurs because of internal reflection in the film around the bright spot at the center of a transform. Plus-x pan 4147 film was used in the photography of the burn patterns, which were then further reduced on EN-7. There is no evidence that grain size limited the expression of the higher frequencies in the transparencies used in the optical processing. Instant film type 55/positive-negative was used for recording the transforms.

The production of the transparencies involved two steps: the making of a negative and the printing of the transparency. Each involved the visual focus of a reduced image, and errors in focus resulted in loss of resolution or contrast in the higher spatial frequencies. The transforms reveal the higher frequencies to be down 2 or 3 orders of magnitude where they might be expected to be down only 1 or 2. A spatial frequency that diffracted 5% of the energy out of the main lobe would be expected to have an amplitude that was 5% of the overall amplitude of the beam.
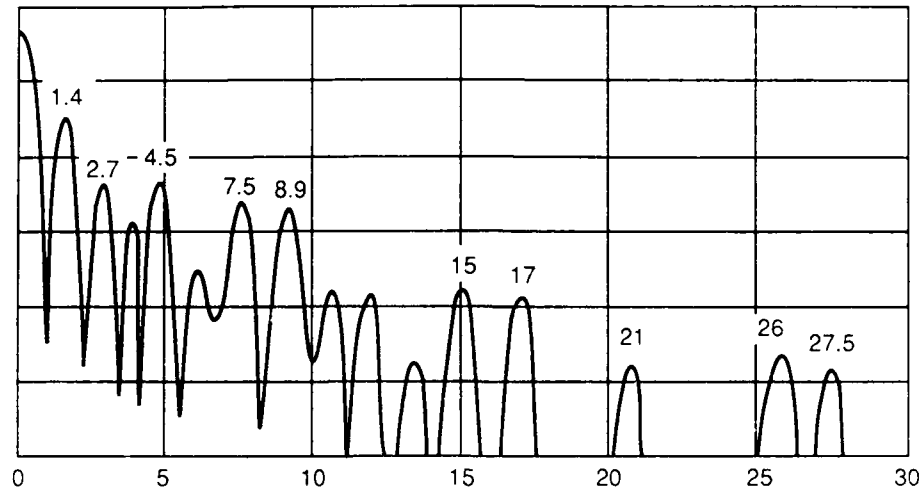
7

Fig. 10 — A sketch of how the vertical spectrum of the optical transform of HL1-093 might look if plotted on a log scale
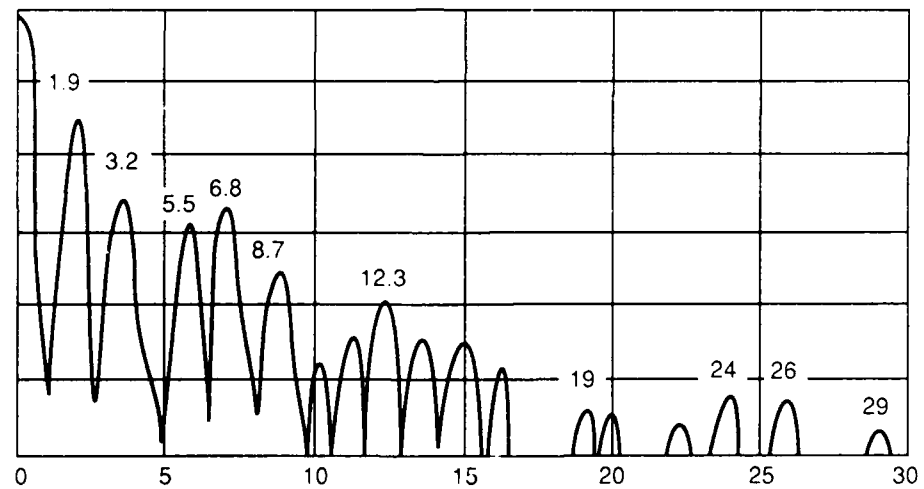

Fig. 11 — A sketch of how the vertical spectrum of the optical transform of ML4 might look if plotted on a log scale

The transparencies have two sources of nonlinearity. One is the apparent density of the tea, which increases exponentially with depth to the point of extinction, and the other is the gamma of the film. The gammas of most films are reasonably linear over the first order of magnitude, which is sufficient here. The nonlinearity introduces harmonics but only in the lower frequencies of the 0 to 2 lines per 14-cm range since only these frequencies have sufficient amplitude to encounter the gross nonlinearity. The most prominent harmonics caused by nonlinearity would be the lower harmonics, and there is no clear evidence of these.

Random errors in the digitization process tend to increase the high-frequency content and have the opposite effect from error in photographic focus. Largely from the low sampling rate, it may be concluded that in this case, the optical transforms are more accurate than the digital one.

DISCUSSION

This analysis was originally undertaken as a minor effort to find clues to the factors that determine the MIRACL beam quality. No remarkable discoveries were made, although the presence of the D_2 feed-hole serpentine frequency was found as it was in other studies. When the second burn pattern became available, the effort was renewed in the hope that it might define the change. What was discovered was that change in the location of the burn combined with the complexity of the MIRACL optical system made comparison difficult. The digitized pattern was explored as a means of comparison to computations of expected patterns, but this proved to be beyond the capability of simple codes. It was also found that the digitization sample rate was too low.

Comparisons of the transforms of the two burn patterns such as Fig. 2 to Fig. 5 or Fig. 10 to Fig. 11 show at least one distinct difference. Frequencies in the range of 18 to 32 lines per 14 cm are more numerous in the second burn than in the first. This suggests that tilting the module banks did spread the wakes into series of ripples where there had been prominent features before.

Burn pattern analysis shows promise as a diagnostic for high energy laser beams. Care should be taken in the choice of location of the burn, and problems such as linearity and sample rate are solvable. For this study, the burn pattern was photographed by time exposure while the light source was moved about to reduce the effect of shadows. A better method might involve the use of a beam splitter so that the pattern could be illuminated from the direction of the camera. The rubber mold of the burn is translucent, and an alternative to immersion in tea might be to illuminate the rubber mold from behind. To digitize a burn, the mold in tea might be imaged with a TV camera and captured by a frame grabber for use in computation. In this case a stair-step scale could be in included in the tea so that the nonlinearity could be corrected digitally.

BLAZER is a comprehensive code by Bullock et al. [3]. A brief description of BLAZER also appears in Gross and Bott [4]. An empty cavity computation of the beam at the burn location by a code such as BLAZER would be helpful in distinguishing those features of the burn caused by diffracting edges from those caused by the character of the gain medium.

Simple calculations of the diffraction from the edges of square apertures (the Appendix) suggest that the phase variation in the beam is less than an eighth wave and that the spatial frequencies of the phase variation are similar to those of the intensity at any given location in the near field. Since these wavelengths vary with distance into the near field, it suggests that the optimum location for a deformable mirror to correct phase would be far enough into the near field that the wavelength should encompass at least two actuators in the mirror. For the MIRACL, the phase data from the BLAZER code would be useful in determining this location.

ACKNOWLEDGMENTS

REFERENCES

1. R. Bracewell, *The Fourier Transform and Its Applications* (McGraw-Hill, New York, 1965).

2. J. W. Goodman, *Introduction to Fourier Optics* (McGraw-Hill, San Francisco, 1968).

3. D. L. Bullock, R. J. Wagner, and R. S. Lipkis, "New Unstable Resonator Program," Report 00173-2-006447, TRW Systems Group, Los Angeles, California, 30 Nov. 1973.

4. R. W. F. Gross and J. F. Bott, *Handbook of Chemical Lasers* (John Wiley & Sons, New York, 1976).

Appendix

The cross sections of the near field at various ranges from a 14-cm-square aperture illuminated with radiation of 3.8 μm wavelength have been calculated. The intensity of the cross section was then transformed to obtain its spatial frequency spectrum. In general, the shorter range cross sections had more of the higher frequencies than did the longer range cross sections.

The even illumination of the aperture was given a sinusoidal phase variation of 0.4 radian peak to peak (~π/8) at a spatial frequency of 15 lines per 14 cm, and then the near field and its spectrum were calculated at 49 and 101 m. Figures A1 and A2, respectively, show the results. Note that the phase modulation is strongly present in the spectra of both ranges into the near field.

In Figs. A1 and A2, line 4 is the phase of the near field. In the left half of the figures, the phase variation is of the order of π/8. In the right half of the figures, outside the beam where the intensity has dropped to zero, the phase jumps meaninglessly between + and −π/2.
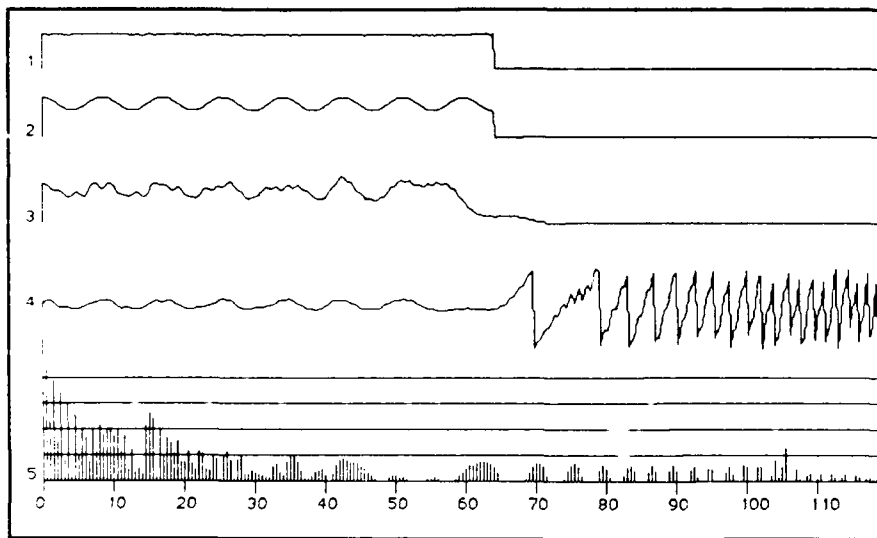

Fig. A1 — One half the cross sections of a 14-cm-wide aperture and its near field at 49 m. Line 1 is the intensity of the 3.8-μm illumination of the aperture, and line 2 is the variation in phase front. Line 3 is the intensity of the near field, and line 4 is the near field phase. Line 5 is the log of the spectrum of the near field intensity in lines per 14 cm, where the Nyquist frequency is 250 lines per 14 cm
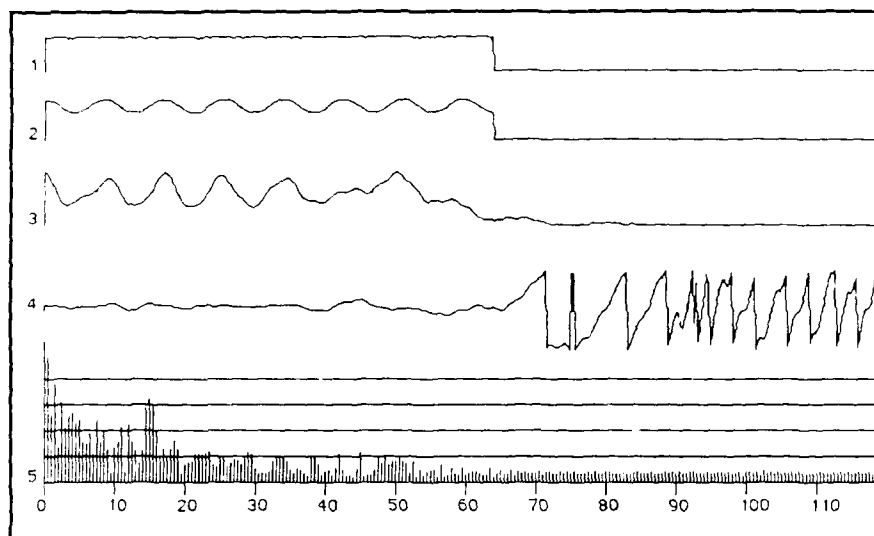
11

Fig. A2 — Similar to Fig. A1, but the near field is at 101 m